

Model-free fault detection and isolation in large-scale cyber-physical systems

Cesare Alippi, *IEEE Fellow*, Stavros Ntalampiras, and Manuel Roveri

Abstract—Detecting and isolating faults in Cyber-Physical Systems (CPSs), e.g., critical infrastructures, smart buildings/cities and the Internet-of-Things, are tasks that do generally scale badly with the CPS size. This work introduces a model-free Fault Detection and Diagnosis System (FDDS) designed having in mind scalability issues, so as to be able to detect and isolate faults in CPSs characterised by a large number of sensors. Following the model-free approach, the proposed FDDS learns the nominal fault-free conditions of the large-scale CPS autonomously by exploiting the temporal and spatial relationships existing among sensor data. The novelties in this paper reside in a) a clustering method proposed to partition the large-scale CPS into groups of highly correlated sensors in order to grant scalability of the proposed FDDS, and b) the design of model- and fault-free mechanisms to detect and isolate multiple sensor faults, and disambiguate between sensor faults and time variance of the physical phenomenon the cyber layer of CPS inspects.

I. INTRODUCTION

Large-scale Cyber Physical Systems (LCPSs) constitute a fertile research domain of great impact. These systems are typically composed of a very large number of heterogeneous units endowed with sensing, processing, communication and (possibly) actuation abilities. Acquired datastreams may be processed in a centralized, distributed or hierarchical way depending on the needs of the envisaged application(s) and its(their) constrains. Monitoring and control of critical infrastructures, smart buildings/cities, Internet-of-Things [1], [2] represent relevant application scenarios of LCPSs and a significant increase of interconnected objects is expected in the next few years [3].

Unfortunately, when operating in real-world (possibly harsh) environmental conditions the probability of having faults affecting the LCPS increases (as it scales with the increase in system complexity) unless suitable actions are taken into account. In particular, faults at the sensor level of LCPS units might induce erroneous data that, once processed by the envisaged application(s), might lead to wrong decisions or reactions [4]. In this paper we focus on faults affecting the sensors of the LCPS units.

Fault Detection and Diagnosis Systems (FDDSs) [5], i.e., systems aiming at detecting, isolating, identifying and (when possible) accommodating faults [6], [7], have been widely studied in the literature and employed in many different

application scenarios (see [8] for a comprehensive review). Unfortunately, FDDSs proposed in the literature mostly consider CPSs characterized by a small-medium number of sensors and suggest solutions that typically do not scale well with CPS size. In addition, most of existing FDDSs

- assume the availability of an a-priori (physical) model for the system under observation, information hardly available in large-scale systems;
- assume the single sensor fault hypothesis that hardly holds when a large number of sensors is considered;
- consider that time variance in the physical phenomenon under inspection affects, if present, all the sensors of the CPS.

Even though a detailed analysis of existing literature is given in Section II, we comment here that available FDDSs for LCPSs rarely consider more than 15 sensors and, as such, it is improper to consider them large-scale systems.

Inspired by [6], [9], [10], this work proposes a novel model-free approach for FDDSs able to manage multiple faults and disambiguate between faults and time variance in the physical process under inspection (representing the physical layer of the LCPS). Unlike traditional FDDSs, a model-free approach does not assume the availability of (analytical) models describing the system under observation neither in nominal nor faulty conditions. The motivation behind considering such an approach comes from the fact that analytical models (whenever available) might not be accurate enough in LCPSs for fault detection/diagnosis purposes and/or their execution might be computationally demanding in large-scale systems, hence not supporting real-time diagnosis. The main characteristics of model-free FDDSs reside in their ability to autonomously learn both the nominal conditions of the system under inspection and the fault dictionary from acquired data during the operational life.

The proposed model-free system for fault detection and isolation in LCPSs relies on a preliminary clustering phase based on a novel correlation-driven clustering algorithm that groups sensors according to the temporal and spatial relationships existing among acquired sensor data. In this way the complexity of designing fault detection and isolation mechanisms for LCPSs reduces by focusing on each cluster of sensors, thus scalability is implemented. Afterwards, for each cluster of sensors, a Hidden Markov Model (HMM)-based mechanism operating both at the single unit and the cluster of units level, inspects incoming datastreams for multiple fault detection and isolation as well as disambiguates faults from time variance affecting the physical layer of the LCPS.

We emphasize that the proposed correlation-based clustering

The authors are with the Dipartimento di Elettronica, Informazione e Bioingegneria, Politecnico di Milano, Milan, Italy, 20133 IT. Prof. Cesare Alippi is also with Università della Svizzera italiana, Switzerland, e-mail: {cesare.alippi,stavros.ntalampiras,manuel.roveri}@polimi.it (see <http://sagroup.ws.dei.polimi.it>).

algorithm is able to operate on heterogeneous sensors (i.e., sensors transducing different physical quantities). This is a relevant progress in the datastream-clustering field (e.g., see [11]) where solutions typically assume time-series coming from homogeneous sensors. The effectiveness and efficiency of the proposed FDDS have been experimentally evaluated on synthetic and real-world datasets coming from rock-collapse monitoring and WiFi Network Management applications.

The paper is organized as follows. Section II analyses the related literature, while the considered problem is formulated in Section III. A general overview of the proposed FDDS along with the proposed clustering algorithm are described in Section IV. The model-free fault detection and isolation mechanisms are detailed in Section V. Experimental results are given in Section VI.

II. RELATED LITERATURE

The literature groups FDDSs into *model-based* and *model-free* methods.

A. Model-based methods

Most of existing works for fault detection/diagnosis in CPSs request the availability of analytical models describing the physical process under investigation [12]–[16].

In this direction, [12] proposes a decentralized method for detecting and isolating multiple sensor faults in large-scale systems based on observers (agents) monitoring subsets of sensors. The detection of faults by each observer is based on an adaptive threshold on the residual, i.e., the discrepancy between what predicted by the a-priori known model and the acquired measurements. There, multiple-fault detection is achieved thanks to an aggregation mechanism that processes decisions gathered by all the observers. The considered application is a robotic-manipulator system encompassing eight sensors. Similarly, a nonlinear model-based observer method for detection, isolation and identification of multiple faults affecting actuators and sensors is proposed in [13]. In this work a simulated waste water-treatment system endowed with six sensors and four actuators has been considered. A similar work is described in [14], and applied to a three-tank system with six sensors and two actuators.

A different approach is presented in [15] that relies on the analysis of the residuals for sensor fault detection and isolation. This method has been applied to a non-isothermal continuous stirred tank reactor and a ternary distillation column envisaging nine sensors. An analytical redundancy-based approach is proposed in [16] that also works on residuals for fault detection and isolation. The experimental campaign includes synthetic data derived from a three-tank system endowed with five sensors and two actuators. In [17], the authors designed a hybrid Kalman filter integrating a mathematical model of the system and a number of piecewise linear (PWL) models. Fault detection is achieved by interpolating the PWL models using a Bayesian approach. Their method is applied on a dataset coming from a simulated gas turbine engine with five sensors.

B. Model-free methods

A contained literature for model-free fault detection/diagnosis is available [18]–[22]. These solutions generally rely on machine-learning or statistical mechanisms to infer a model for the system under inspection directly from data.

For example, a method based on Auto-Regressive with eXogenous input (ARX) model to characterize time-invariant relationships between sensors is presented in [19]. There, fault detection relies on the analysis of residuals, while fault isolation employs a graph-based analysis to identify anomalous patterns. The considered dataset refers to a physical plant containing 1091 sensors. There, the case of heterogeneous sensors is not considered, and time invariance for the plant under inspection is assumed.

A data-driven method based on Principal Component Analysis (PCA) and Fisher discriminant analysis to diagnose multiple faults is presented in [20]. PCA is applied to raw data for detecting anomalies by checking residuals, while Fisher discriminant analysis isolates the faults. The application refers to an air-handling unit composed of 13 sensors. An adaptive monitoring method based on residuals coming from a sliding window is presented in [21]. The method is applied to a real air-compression process monitored by 8 sensors.

Neural networks have been often considered in model-free solutions to model the unknown physical process. For example, [22] considers Artificial Neural Networks to identify and isolate multiple faults in an industrial motor network composed of 6 sensors. There, the fault dictionary is assumed to be a-priori available. Finally, a swarm intelligent-based approach for the diagnosis of multiple faults is proposed in [18]. The fault diagnosis problem is modified so that the presence (or absence) of a specific fault is associated to each vertex explored by an ant. The experimental framework considers an industrial remote monitoring of operating machines with 20 sensors.

III. PROBLEM DESCRIPTION

Let us consider a LCPS composed by a set $\mathcal{S} = \{s^1, \dots, s^N\}$ of N sensors monitoring an unknown and, possibly, time-varying process \mathcal{P} . Sensors in \mathcal{S} can be homogeneous (measuring the same physical quantity) or heterogeneous (measuring different but related physical quantities).

At each time instant t , sensors in \mathcal{S} provide the measurement vector $X_t = [x_t^1, \dots, x_t^N]$, where $x_t^i \in \mathbb{R}$ is the scalar measurement acquired at time t by sensor s^i . Without loss of generality sensors in \mathcal{S} are assumed to be synchronous and sampled with the same sampling frequency.

We assume that \mathcal{P} is initially stationary since time variance typically occurs only later on in time. During the operational life sensors in \mathcal{S} might be affected by faults so that, for the generic sensor s^i affected by a fault at time t_i^* , the datastream x_t^i s is perturbed as follows

$$x_t^i = \begin{cases} x_t^i & t < t_i^* \\ \phi(x_t^i) & t \geq t_i^* \end{cases} \quad (1)$$

where $\phi(\cdot)$ represents the (possibly nonlinear) fault function, which is characterized by a time profile and a signature [8] of

the fault. The former refers to the fault-time duration, e.g., permanent, transient or intermittent, and the fault-evolution model, e.g., abrupt or incipient; the latter characterizes the type of fault, such as offset, drift or precision degradation. Here, we permit the CPS to be affected by concurrent multiple sensor faults.

We model time variance as a change in \mathcal{P} , i.e., the system model evolves from \mathcal{P} to \mathcal{P}' at an unknown time instant t_p^* . Disambiguation between faults and time variance is an important ability for the FDDS since the LCPS might need to react in different ways to the change, e.g., as presented in [23].

The proposed FDDS for LCPSs inspects data acquired by \mathcal{S} to promptly *detect* and *isolate* multiple changes as seen at the readout of the sensors, as well as disambiguate between *faults* and *time variance*. We emphasize that the proposed FDDS is independent from the specific network topology or implemented routing protocol.

IV. THE PROPOSED MODEL-FREE FAULT DETECTION AND DIAGNOSIS SYSTEM

In this section we introduce the proposed FDDS for LCPSs, whose general architecture is given in Fig. 1. The key idea of the proposed solution resides in its ability to model the relationships existing among acquired sensor datastreams x_t^i s and autonomously learn the nominal (fault-free) conditions of \mathcal{P} . Faults and time variance are then perceived as deviations from these nominal conditions.

This is a crucial aspect in the proposed model-free solution since the sensors of the LCPS open different but related views of the same physical phenomenon, thus time variance in \mathcal{P} would affect a set of (highly) correlated sensors allowing us to discriminate between faults and time variance in \mathcal{P} . As such, we do not assume that time variance in the LCPS is perceived by all sensors in \mathcal{S} .

As shown in Fig. 1, the proposed FDDS requires the following steps:

- 1) cluster sensors $\{s^1, \dots, s^N\}$ according to the functional relationships existing among datastreams $\{x_t^1, \dots, x_t^N\}$, $t = 1, 2, \dots$ by means of a novel clustering algorithm based on the k -medoids clustering mechanism complemented with a pairwise-dissimilarity metric based on cross-correlation;
- 2) build a HMM-based change detection mechanism for each cluster so as to detect variations w.r.t. the learned nominal conditions of \mathcal{P} ;
- 3) execute the change detection mechanism during the operational life and, if a change is detected, disambiguate between sensor faults (and, in this case, isolate the affected sensors) and time variance in \mathcal{P} .

The proposed FDDS requires the availability of a training set TS encompassing data acquired by all sensors for the first T time instances:

$$TS = \begin{bmatrix} x_1^1 & \dots & x_T^1 \\ \vdots & \ddots & \vdots \\ x_1^N & \dots & x_T^N \end{bmatrix}, \quad (2)$$

Input: TS, ν_{max}, I_{max} ;

1. Create T_{ts}, V_{ts} as in Eq. 3 ;
 2. Initialize $e_{tot} = []$;
 3. **for** $\nu = 1 : \nu_{max}$ **do**
 4. Apply k -medoids algorithm I_{max} times on T_{ts} and get $C^\nu = \{C^1, \dots, C^\nu\}$;
 5. **if** $checkIsolation=true$ **then**
 - Go to next clustering setting, $\nu=\nu+1$;
 - end**
 6. Initialize $e_{val}^\nu = []$;
 7. **for** $j=1:\nu$ **do**
 8. $e_i = 0$;
 9. **for** $i=1:|C^j|$ **do**
 - Create MISO model $\mathcal{M}_{i,j}^\ominus$ using T_{ts} ;
 - Compute the error of $\mathcal{M}_{i,j}^\ominus$ on V_{ts} and denote it as $e_{V_{ts}}^i$;
 - $e_i = e_i + e_{V_{ts}}^i$
 - end**
 10. $e_{val}^\nu = [e_{val}^\nu; e_i/|C^i|]$
 - end**
 11. $e_{tot} = [e_{tot}; sum(e_{val}^\nu)/\nu]$;
 - end**
 12. Find $min(e_{tot})$ and identify its index;
- Output: ν_0 ;

Algorithm 1: The algorithm for clustering N datastreams.

that is assumed to be both time invariant and fault-free (neither faults nor changes in \mathcal{P} have occurred up to time T). TS is used to configure the proposed FDDS.

A. Sensor Clustering in Large-Scale Cyber-Physical System

A novel cross-correlation-based clustering algorithm inspired by the k -medoids clustering mechanism [24] is proposed to cluster sensors in \mathcal{S} based solely on the functional relationships existing among datastreams x_t^i s. This is a crucial difference w.r.t. datastream clustering solutions, e.g., [11], which generally consider time-series coming from homogeneous sensors. It should be highlighted that an algorithm able to process datastreams coming from heterogeneous sensors is necessary in the context of CPSs (and even more with LCPSs), where assuming homogeneous sensors is not realistic.

B. The k -mediods algorithm

The main characteristic of the k -mediods clustering algorithm is its ability to incorporate the more general concept of *pairwise dissimilarity* as a metric, rather than the Euclidean one (as done in the traditional k -means algorithm). This guarantees a more robust clustering phase since the effects of outliers reduce significantly [24].

The k -mediods algorithm operates as follows: given the number of clusters ν to be considered (which is a user-defined parameter), the algorithm randomly selects ν elements from the set as *medoids*. Then, the algorithm associates each element of the set to the closest medoid and computes the overall sum

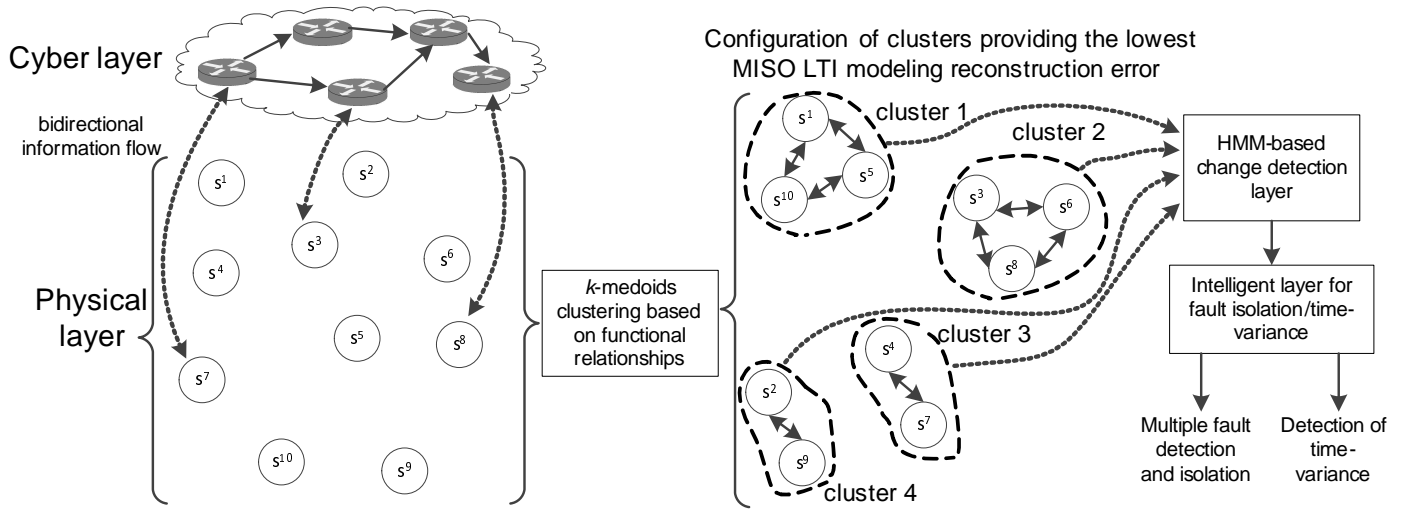


Fig. 1. The general idea of the proposed multiple fault detection and isolation system for LCPSs. After sensors clustering (network partitioning), the proposed algorithm relies on an HMM-based change detection mechanism activating the intelligent layer, when necessary. Isolation of multiple faults and detection of changes in time variance follow.

of pairwise dissimilarities. This procedure, i.e., the random medoids selection and element association to each medoid, is repeated I_{max} iterations and the cluster configuration characterized by lowest sum of pairwise dissimilarities chosen.

In our specific case, the elements to be processed by the k -medoids algorithm are the streams of data in TS , which is divided into training T_{ts} and validation V_{ts} sequence as follows

$$T_{ts} = \begin{bmatrix} x_1^1 & \dots & x_\Lambda^1 \\ \vdots & \ddots & \vdots \\ x_1^N & \dots & x_\Lambda^N \end{bmatrix}, V_{ts} = \begin{bmatrix} x_{\Lambda+1}^1 & \dots & x_T^1 \\ \vdots & \ddots & \vdots \\ x_{\Lambda+1}^N & \dots & x_T^N \end{bmatrix}. \quad (3)$$

T_{ts} is used by the k -medoids algorithm to cluster sensors according to the estimated cross-correlation between the respective datastreams, while V_{ts} is used for identifying the proper number of clusters ν_0 as shown in Alg. 1 and detailed in Section IV-D.

As pairwise-dissimilarity measure $d_{i,j}$, we propose the complement of the cross-correlation between streams of data acquired by sensor s^i and s^j computed on T_{ts}^i and T_{ts}^j (i.e., the i -th and j -th row of T_{ts}) defined as

$$d_{i,j} = 1 - Cor_{\tau_0}(T_{ts}^i, T_{ts}^j), \quad (4)$$

where

$$Cor_{\tau}(T_{ts}^i, T_{ts}^j) = \frac{(T_{ts}^i - \bar{T}_{ts}^i)(T_{ts}^j - \bar{T}_{ts}^j)'}{\sqrt{(T_{ts}^i - \bar{T}_{ts}^i)(T_{ts}^i - \bar{T}_{ts}^i)'}} \sqrt{(T_{ts}^j - \bar{T}_{ts}^j)(T_{ts}^j - \bar{T}_{ts}^j)'}$$

being \bar{T}_{ts}^i and \bar{T}_{ts}^j the average time-series of all datastreams over T_{ts} , while $'$ is the transpose operator. $\tau_0 = \arg\max_{\tau}(Cor_{\tau}(T_{ts}^i, T_{ts}^j))$ represents the time-lag maximising

the cross-correlation between T_{ts}^i and T_{ts}^j . $d_{i,j}$ is bounded, i.e., $0 \leq d_{i,j} \leq 1$. The lower the $d_{i,j}$, the larger the cross-correlation between the respective datastreams. In the proposed FDDS, the implementation of the k -medoids algorithm is based on the Partitioning Around Medoids presented in [25].

C. Modelling the functional relationships of the sensor datastreams in a cluster

As described in the previous section, the outcome of the k -medoids algorithm is a set of ν clusters grouping highly correlated sensors of \mathcal{S} , i.e., $C^{\nu} = \{C_1, \dots, C_{\nu}\}$, where C_j contains the indices of sensors belonging to cluster j . Then, for each cluster $j = 1, \dots, \nu$, we create $|C_j|$ Multiple-Input Single-Output (MISO) predictive models ($|\cdot|$ is the cardinality operator), where the i -th sensor (with $i = 1, \dots, |C_j|$) belonging to cluster j represents the single-output and the remaining $|C_j| - 1$ sensors represent the inputs¹.

For this purpose, we rely on the Input-Output MISO predictive model $g^{i,j}$:

$$\hat{x}_t^{i,j} = g^{i,j}(x_{t-1}^{i,j}, x_{t-2}^{i,j}, \dots, x_{t-\tau}^{i,j}, x_t^{1,j}, x_{t-1}^{1,j}, \dots, x_{t-\tau}^{1,j}, \dots, x_t^{|C_j|,j}, x_{t-1}^{|C_j|,j}, \dots, x_{t-\tau}^{|C_j|,j}, \hat{\Theta}) \quad (5)$$

where the parameter vector $\hat{\Theta}$ and τ are suitably estimated on the rows of T_{ts} referring to the sensors belonging to cluster j .

In this work we consider the specific case where $g^{i,j}$ is linear. Linear models are characterized by a contained computational complexity and are particularly appropriate whenever the physical process investigated by the LCPS is ruled by linear

¹In principle we might also consider overlapping subsets of sensors, if useful to the fault detection/isolation purposes.

ordinary differential equations, a situation that represents a first order model for many physical systems. Among the linear input-output MISO predictive models [26], we considered Auto-Regressive with eXogenous input (ARX) models, here defined in vectorial form as

$$\hat{x}_t^{i,j} = \langle [x_{t-1}^{i,j}, \dots, x_{t-\tau}^{i,j}], \Theta \rangle \quad (6)$$

where $\Theta = [\theta_1, \dots, \theta_u]$ is the vector of model parameters (being u the cardinality of vector $[x_{t-1}^{i,j}, \dots, x_{t-\tau}^{i,j}]$) and $\langle \cdot \rangle$ the scalar product operator. We stress out the fact that using linear models is not a restrictive choice since we are not specifically interested in the prediction accuracy of the model but, instead, in opening a view on the relationships existing among sensors.

To ease the notation, we refer in the sequel $M_{\Theta}^{i,j}$ to be the ARX predictive model of the i -th sensor belonging to the j -th cluster. The associated parameter vector $\hat{\Theta}^{i,j}$ s represents the information requested by the HMM-based mechanisms for fault detection and isolation described in Section V.

D. Discovering the optimal number of clusters

One crucial limitation of the traditional k -medioids algorithm, as described in Section IV-B, is the fact that the number of clusters ν must be provided. To overcome this limit we introduce a solution to select the proper number of clusters ν_0 through an exploration of different values of ν . The selection criterion is based on evaluating the ability of the estimated models $M_{\Theta}^{i,j}$ s in Eq. (6) upon effectively capturing the relationships existing among the acquired datastreams within each cluster.

More specifically, given $\mathcal{C}^{\nu} = \{C_1, \dots, C_{\nu}\}$ the set of clusters provided as output by the k -medioids algorithm given ν (line 4, Alg. 1), we compute the overall reconstruction error e_{val}^{ν} of $M_{\Theta}^{i,j}$ s on V_{ts} (lines 6-10, Alg. 1). Denote the predictions of model $M_{\Theta}^{i,j}$ on V_{ts} as $Y_V^{i,j}$ and let $e_{i,j}$ be the reconstruction error measuring the differences between V_{ts} and $Y_V^{i,j}$. The overall reconstruction error is calculated as

$e_{val}^{\nu} = \frac{1}{\nu} \sum_{j=1}^{\nu} \frac{1}{|C_j|} \sum_{i=1}^{|C_j|} e_{i,j}$. We emphasize that e_{val}^{ν} measures how well the estimated ARX models in Eq. 6 given the clusterization $\mathcal{C}^{\nu} = \{C_1, \dots, C_{\nu}\}$, are able to effectively predict the datastreams in V_{ts} .

The optimal number of cluster ν_0 is chosen (lines 11-12, Alg. 1) as the one minimizing the reconstruction error e_{val}^{ν} on V_{ts}

$$\nu_0 = \underset{1 < \nu < \nu_{max}}{\operatorname{argmin}} (e_{val}^{\nu}), \quad (7)$$

where ν_{max} is a user-defined parameter. In order to create the MISO ARX models in Eq. (6), the clusters settings \mathcal{C}^{ν} s characterized by one or more clusters with isolated sensors (i.e., clusters composed by just one sensor) are discarded² (line

²It should be noted that two normalization processes are involved in order to compare the considered cluster sets. The former refers to the MISO models where the sum of errors e_i is normalized by the number of sensors $|C_j|$ included in the specific cluster j . The latter refers to the cluster level where the sum of errors e_{val}^{ν} is normalized w.r.t. the number of clusters ν .

5 of Alg. 1).

The final outcome of the proposed correlation-based clustering algorithm is the set of ν^0 clusters, i.e., $\mathcal{C}^{\nu^0} = \{C_1, \dots, C_{\nu^0}\}$.

V. HMM-BASED MECHANISMS FOR FAULT DETECTION AND ISOLATION

The proposed FDDS is organized as a two-layer architecture where the lower layer encompasses the HMM-based mechanisms for change detection while the upper one disambiguates changes between faults and time variance and, subsequently, isolates the faults (whenever they occur).

A. HMM-based change detection layer

The considered HMM-based change detection mechanism [6], [27] aims at monitoring the evolution over time of parameter $\hat{\Theta}^{i,j}$ s estimated on the MISO models defined in Eq. 6 through a Hidden Markov Model. Vector parameters $\hat{\Theta}^{i,j}$ are estimated on overlapping windows of size w and step h . The HMM-based change detection mechanism requires the training of a HMM characterizing the stationary conditions. Variations w.r.t. these conditions are perceived as changes in the statistical behaviour of estimated parameters $\hat{\Theta}^{i,j}$, hence requiring a further analysis to discriminate between faults and time variance, and isolate the faults.

In more detail, a HMM $H^{i,j}$ operating on $M_{\Theta}^{i,j}$ is defined by $\{S, P(\Theta^{i,j}|\Phi), A, \pi\}$, where S is the number of states, P the pdf of each state, Φ comprises the set of values $[\mu, \sigma]$ characterizing the Gaussian mixture of each state, A is the state transition matrix, π the initial state distribution. The HMM-based change detection mechanism first trains $H_{i,j}$ on the fault-free training sequence of estimated parameters $\hat{\Theta}^{i,j}$ s computed on V_{ts} (line 1 of Alg. 2). Afterwards, at time t during the operational life of the FDDS, the parameters estimated on the incoming data are provided to the HMM $H_{i,j}$ and their statistical compatibility is measured in terms of log-likelihood $L_t^{i,j}$ (line 3 of Alg. 2). If the log-likelihood $L_t^{i,j}$ falls below an automatically-defined threshold $T_h^{i,j}$ (computed as described in [6]), a change in the MISO model $M_{\Theta}^{i,j}$ is detected (lines 4-5 of Alg. 2) and the intelligent level is activated for further processing.

B. Intelligent layer for fault isolation/time-variance

When a change has been detected by a HMM-based change detection mechanism at time t , the intelligent layer is activated to understand whether the specific change corresponds to a fault affecting one of the sensors of the cluster or it represents a time variance in \mathcal{P} .

In more detail, given a detection in the HMM-based change detection mechanism inspecting $M_{\Theta}^{\bar{i},\bar{j}}$, i.e., corresponding to the \bar{i} -th sensor of the \bar{j} -th cluster, the intelligent level gathers the log-likelihoods $L_t^{\bar{j}}$ produced by the HMM change detection mechanisms of the other sensors in cluster \bar{j} at time t , i.e. $L_t^{\bar{j}} = [L_t^{1,\bar{j}}, \dots, L_t^{|\mathcal{C}_{\bar{j}}|-1,\bar{j}}]$, as well as the corresponding thresholds, i.e. $T_h^{\bar{j}} = [T_h^{1,\bar{j}}, \dots, T_h^{|\mathcal{C}_{\bar{j}}|-1,\bar{j}}]$ (line 2, Alg. 3).

Input: V_{ts}, w, h, i, j ;

1. Generate HMM, $H^{i,j} = \{S, P, A, \pi\}$ on $\hat{\Theta}^{i,j}$ s estimated on V_{ts} windowed using length w overlapping by h and compute the threshold $T_h^{i,j}$ as described in [6]; **while** (Incoming data are available at time t) **do**
 2. Compute the parameter vector $\hat{\Theta}^{i,j}$ of the prediction model $M_{\Theta}^{i,j}$;
 3. Compute the log-likelihood $L_t^{i,j}$ of $\hat{\Theta}^{i,j}$ s given $H^{i,j}$;
 - if** $L_t^{i,j} < T_h^{i,j}$ **then**
 4. Change detected in $M_{\Theta}^{i,j}$;
 5. Activate the fault isolation/time-variance layer;
- end**

Algorithm 2: The HMM-based Change Detection mechanism.

Input: Detection at sensor \bar{i} of cluster \bar{j} , $H^{i,\bar{j}}$, $i = 1, \dots, |C_{\bar{j}}|$;

1. HMM-based change detection mechanism associated with $H^{i,\bar{j}}$, $i = 1, \dots, |C_{\bar{j}}|$, detected a change at time t ;
 2. Gather $L_t^{\bar{j}} = [L_t^{1,\bar{j}}, \dots, L_t^{|\bar{C}_{\bar{j}}|-1,\bar{j}}]$ and $T_h^{\bar{j}} = [T_h^{1,\bar{j}}, \dots, T_h^{|\bar{C}_{\bar{j}}|-1,\bar{j}}]$;
 3. Compute the average values at the cluster level, i.e.
$$\bar{T}_t^{\bar{j}} = \frac{1}{|C_{\bar{j}}|-1} \sum_{i=1, i \neq \bar{i}}^{|\bar{C}_{\bar{j}}|} T_h^i, \bar{L}_t^{\bar{j}} = \frac{1}{|C_{\bar{j}}|-1} \sum_{i=1, i \neq \bar{i}}^{|\bar{C}_{\bar{j}}|} L_t^i ;$$
 4. **if** $\bar{L}_t^{\bar{j}} < a\bar{T}_t^{\bar{j}}$ **then**
 - | Time-variance at cluster \bar{j} ;
 - else**
 - | Fault detected at sensor $s^{\bar{i},\bar{j}}$;
- end**
- Output: Fault isolation at $s^{\bar{i},\bar{j}}$ or time variance detection at cluster \bar{j} ;

Algorithm 3: The considered HMM-based mechanism for fault isolation/time variance.

The intelligent layer analyses the likelihoods $L_t^{\bar{j}}$ and thresholds $T_h^{\bar{j}}$ as follows: it computes the average values of the thresholds $T_h^{\bar{j}}$ and log-likelihoods $L_t^{\bar{j}}$ associated with cluster \bar{j} , i.e. $\bar{T}_t^{\bar{j}} = \frac{1}{|C_{\bar{j}}|-1} \sum_{i=1, i \neq \bar{i}}^{|\bar{C}_{\bar{j}}|} T_h^i$, $\bar{L}_t^{\bar{j}} = \frac{1}{|C_{\bar{j}}|-1} \sum_{i=1, i \neq \bar{i}}^{|\bar{C}_{\bar{j}}|} L_t^i$, (line 3, Alg. 3). When $\bar{L}_t^{\bar{j}} < a\bar{T}_t^{\bar{j}}$ (line 4, Alg. 3), the intelligent layer signals a time variance perceived in cluster \bar{j} since all sensors in cluster \bar{j} are perceiving a variation in their statistical behaviour (possibly with different magnitudes or signatures). The correcting factor a is a user-defined parameter incorporating domain-expert knowledge (water supply system, communication network, etc.). On the contrary, when $\bar{L}_t^{\bar{j}} > a\bar{T}_t^{\bar{j}}$, the intelligent layer associates the change to a fault affecting sensor \bar{i} of cluster \bar{j} .

VI. EXPERIMENTS

The aim of this section is to experimentally validate the effectiveness of the proposed FDDS for LCPSs dealing with multiple faults and time variance. To achieve this goal we consider a synthetic experiment and two datasets coming from real-world LCPSs, i.e., a rock-collapse and landslide monitoring system deployed on the Italian Alps [28] and the WiFi network of a large university in northern Italy (Politecnico di Milano).

A. The synthetic experiment and the real-world datasets

The synthetic experiment: The generation of the synthetic dataset comprises two steps. At first, we generate streams of data by using a cosine function with period 5π corrupted by the zero-mean Gaussian noise $\eta \sim G(0, 0.5)$. In the second step we generate the N datastreams x_t^i , $i = 1, \dots, N$ according to the ARX(2,2) models:

$$x_t^i = a_1^i x_{t-1}^i + a_2^i x_{t-2}^i + b_1^i x_{t-1}^j + b_2^i x_{t-2}^j + \eta \quad (8)$$

where $a_1^i, a_2^i, b_1^i, b_2^i$ are randomly drawn from a uniform distribution $U = [0, 2]$ and x_t^j s refer to the previously generated datastream. Each experiment lasts 8000 samples with the first $T = 5000$ samples used for training. We considered two different scales of the LCPS, i.e., $N = \{30, 50\}$.

The real-world LCPSs: The first real-world application refers to a rock collapse and landslide forecasting system, where a hybrid wireless-wired monitoring system gathers data from a mountain environment to forecast (possible) rock collapses [28], [29]. The system, which has been deployed on the Italian Alps, encompasses $N = 13$ sensors (6 temperature, 4 clinometer and 3 crackmeter sensors). The considered dataset³ lasts 2844 samples, while the sampling period is 1h. Here, the first $T = 1500$ samples are used for training the FDDS.

The second real-world LCPS refers to the WiFi network. More specifically, the considered dataset refers to the uplink-traffic (WiFi-U) and downlink-traffic (WiFi-D) measurements recorded by 28 hot spots measuring the upload and download traffic within the University in October 2015 leading to 56 datastreams (virtual sensors), whose length is 4000 samples. The first $T = 2500$ samples are used for training, while the sampling period is 5 minutes.

B. Fault and time-variance modelling

In order to quantitatively assess the performance of the proposed FDDS, we artificially injected multiple faults and time variance in both the synthetically-generated and the real-world datasets.

As regards the multiple faults, we randomly select a subset S_f of sensors in \mathcal{S} , where the cardinality of S_f ranges from 5% to 15% of N . Then we artificially inject a perturbation on sensors in S_f at time t^* . Here, two kinds of perturbations are considered; for the generic sensor i in s_f

³The dataset can be downloaded at the following URL <http://roveri.faculty.polimi.it/software-and-datasets/>

- stuck-at,

$$x_t^i = \begin{cases} x_t^i & t < t^* \\ x_{t^*}^i, & t \geq t^*, \end{cases} \quad (9)$$

- abrupt multiplicative,

$$x_t^i = \begin{cases} x_t^i & t < t^* \\ \alpha x_{t^*}^i, & t \geq t^*, \end{cases} \quad (10)$$

where $\alpha = \{0.15, 0.3\}$. These fault models represent two large classes of real-world faults: the stuck-at refers to a sensor malfunction where the sensor output is stuck over time to a fixed value, while the abrupt multiplicative one refers to a fault affecting, in an abrupt way, the calibration of the sensor [30]. In the synthetic dataset, we consider $t_i^* = 7000$; in the rock-collapse and landslide monitoring system $t_i^* = 2644$, while in the WiFi network $t_i^* = 3500$.

Differently, time variance is modelled by a) randomly choosing a sensor in \mathcal{S} , b) sorting all the other sensors in \mathcal{S} according to the cross-correlation on the respective datastreams in TS , and c) selecting those sensors characterized by the largest cross-correlation values. In particular, we considered three configurations for time variance where the number of selected sensors is $\{30\%, 50\%, 70\%\}$ of N . Once the subset of sensors has been selected, time variance is introduced by changing the ARX parameters of respective models (Eq. 8) from $\theta = \{a_1, a_2, b_1, b_2\}$ to $\theta_\lambda = \{a_1(1+\lambda), a_2(1+\lambda), b_1(1+\lambda), b_2(1+\lambda)\}$, where λ ranges from 0.05 to 0.1. The change in the time variance starts at the time instant $t_p^* = 7000$.

The simulation results associated with the synthetically-generated data are averaged over 100 runs.

C. Proposed solution

The proposed FDDS has been configured as follows. The HMM considered by the HMM change detection mechanisms has been set according to a fully connected topology (ergodic HMMs). The number of states of the HMM is selected from the set $\{3, 4, 5, 6\}$, while the number of Gaussian functions⁴ from the set $\{2, 4, 8, 16, 32, 64, 128\}$. Models $M_{\Theta}^{i,j}$ s are selected through a search performed in the validation set V_{ts} . The autoregressive and exogenous component orders of (5) are identified on V_{ts} in the range 1 to 6, while $I_{max} = 200$. The frame length w of the HMM change detection mechanism is set to 100 with $h = 1$ except for the WLAN dataset, where $w = 1000$ and $h = 1$.

The proposed FDDS is contrasted with the solution presented in [6], where no clustering mechanism is considered and relationships among sensor datastreams are modelled through SISO predictive models. [6] was selected as, at present, there does not exist any FDDS in the literature for LCPSs able to deal with time variance in \mathcal{P} .

⁴It should be noted that the state search for the HMM which explains at best the datastream is performed only at the cluster head coordinating the cluster of units, i.e., the sensor with the minimum distance defined in Eq. (4) with respect to all the sensors belonging to the cluster.

D. Figures of merit

To measure the ability to promptly detect and correctly recognize the occurrence of multiple faults/time variance, we consider the following four figures of merit:

- 1) False Positive (FP): it measures the times a change is detected by the FDDS, while it is not present. In case of multiple-faults, a FP occurs either when a change is detected in sensor s^i before t_i^* or in a sensor that has not been affected by the fault. In case of time-variance, a FP occurs when the change is detected either before t_i^* or in a sensor not affected by the time variance procedure as described in Section VI-B.
- 2) False Negative (FN): it counts the number of times that the proposed FDDS does not detect all existing faults/time variance changes.
- 3) Detection Delay (DD): it measures the time delay (in number of samples) between when the change started (either the multiple faults or time variance) and the time it is detected by the FDDS.
- 4) Recognition Accuracy (RA): it measures the percentage of experiments where the FDDS is able to correctly isolate all faults and distinguish between faults and time variance in \mathcal{P} .

In addition, we also measured the execution time ET (CPU time). For this purpose, a Server Dell PowerEdge T710 with 24 cores (2.4Ghz) and 48GB of RAM was employed. This allows the reader to quantitatively evaluate the time complexity of the proposed FDDS.

E. Discussions

The experimental results about multiple faults and time variance for both synthetic and real-world datasets are shown in Tables I, II, III and IV, V, VI, respectively.

Several comments arise. First, the proposed FDDS guarantees lower FP, FN, DD and ET than [6] (see columns 2-5 and 7-10 in Tables I-III). As expected, FNs and DDs decrease with the magnitude of the abrupt fault. The stuck-at fault model provides results that are in line or even better than those obtainable in correspondence with the abrupt one, as the stuck-at fault completely changes the dynamics of the acquired datastream, which is reflected in the estimated parameters. It should be emphasized that ETs of the proposed FDDS are significantly lower compared with those of the contrasted solution (this is a relevant aspect when dealing with embedded units of LCPSs) as shown in columns 5 and 10 in Table I-III. Moreover, as expected, ET increases with N since the proposed FDDS requires to process data coming from a larger number of sensors.

Second, the results on the dataset coming from the rock-collapse forecasting application are in line with those obtained with synthetic data (see rows 8-10 in Tables I-III). The proposed FDDS identified two clusters out of the 13 sensors meaning that acquired data are (as expected) related in time and space. Similarly, the results regarding the WLAN data are also encouraging and the superiority of the proposed FDDS is shown with respect to both Uplink and Downlink data (see rows 11-16 of Tables I-III). Even in this case the datastreams

are related in time and space and the number of clusters discovered by the algorithm is two.

Third, FN and DD about time variance in \mathcal{P} are particularly interesting (Tables IV-VI). As expected, the larger the λ the smaller FN and DD. Results provided by the proposed FDDS are significantly better than the ones of the contrasted solutions since the latter relies on one change detection mechanism for each SISO model and this might dramatically increase FP detections. In all the configurations, i.e., $\{30\%, 50\%, 70\%\}$, FN rates are very satisfactory, while DDs are quite low due to the ability of the HMM change detection mechanisms in characterizing the statistical behaviour of the acquired datastreams and providing decreasing log-likelihoods. Interestingly, the contrasted solution is not able to detect the changes affecting only 30% of the sensors since its analysis is carried out by considering the whole set of sensors.

Fourth, the great ability of the proposed FDDS in isolating all faults and distinguishing between multiple faults and time variance is shown by the high RA values (see columns 6, 11 in Tables I-VI). As regards multiple faults, both solutions are effective in distinguishing between faults and time variance (columns 6, 11 in Tables I-III). Differently, in case of time variance, the proposed solution is meaningfully better in recognizing the occurrence of time-variance and distinguishing it from multiple-faults thanks to the cluster level analysis.

VII. CONCLUSIONS

This work proposes a novel model-free FDDS able to operate in LCPSs. It is based on the learning and exploitation of functional relationships existing among the datastreams produced by sensors of the LCPS by means of a novel clustering mechanism. The proposed FDDS relies on HMM change detection mechanisms operating in the space of the coefficients of MISO LTI models and their outcomes are aggregated at the intelligent level, where the proposed FDDS is able to isolate multiple faults and differentiate between faults and time variance in the system under inspection. The performance of the proposed FDDS has been thoroughly evaluated on both synthetic and real-world large-scale datasets.

Future works include the design of the fault identification and accommodation phases. We intent to develop an identification algorithm operating in an *online* manner, i.e., able to automatically create fault models, identify faults in the incoming datastreams, and create/update the fault dictionary. Once the fault/time variance has been verified, the proper accommodation phase will be actuated to reduce the effects of the fault on the system and avoid potentially catastrophic cascade effects (e.g. by using virtual sensors or retrain the models at the cluster level).

ACKNOWLEDGMENT

This work was supported by the project GAUCHO - A Green Adaptive Fog Computing and Networking Architecture under the PRIN initiative PROGETTI DI RICERCA DI RILEVANTE INTERESSE NAZIONALE Bando 2015 Prot. 2015YPXH4W. The authors would like to thank Prof. Matteo Cesana and the ANTLAB for the dataset about the WiFi Network.

REFERENCES

- [1] T. Gibson, S. Ciraci, P. Sharma, C. Allwardt, M. Rice, and B. Akyol, "An integrated security framework for goss power grid analytics platform," in *Dependable Systems and Networks (DSN), 2014 44th Annual IEEE/IFIP International Conference on*, June 2014, pp. 786–791.
- [2] A. Kane, T. Fuhrman, and P. Koopman, "Monitor based oracles for cyber-physical system testing: Practical experience report," in *Dependable Systems and Networks (DSN), 2014 44th Annual IEEE/IFIP International Conference on*, June 2014, pp. 148–155.
- [3] O. Vermesan and P. Friess, Eds., *Internet of Things: From Research and Innovation to Market Deployment*, ser. River Publishers Series in Communication. Aalborg: River, 2014.
- [4] S. Zug, T. Brade, J. Kaiser, and S. Potluri, "An approach supporting fault-propagation analysis for smart sensor systems," in *SAFECOMP Workshops*, ser. Lecture Notes in Computer Science, F. Ortmeier and P. Daniel, Eds., vol. 7613. Springer, 2012, pp. 162–173.
- [5] R. Leon, V. Vittal, and G. Manimaran, "Application of sensor network for secure electric energy infrastructure," *Power Delivery, IEEE Transactions on*, vol. 22, no. 2, pp. 1021–1028, April 2007.
- [6] C. Alippi, S. Ntalampiras, and M. Roveri, "A cognitive fault diagnosis system for distributed sensor networks," *Neural Networks and Learning Systems, IEEE Trans. on*, vol. 24, no. 8, pp. 1213–1226, Aug 2013.
- [7] C. Keliris, M. Polycarpou, and T. Parisini, "A distributed fault detection filtering approach for a class of interconnected continuous-time nonlinear systems," *Automatic Control, IEEE Transactions on*, vol. 58, no. 8, pp. 2032–2047, Aug 2013.
- [8] R. Isermann, *Fault-diagnosis systems: an introduction from fault detection to fault tolerance*. Springer Verlag, 2006.
- [9] H. Chen, P. Tino, A. Rodan, and X. Yao, "Learning in the model space for cognitive fault diagnosis," *Neural Networks and Learning Systems, IEEE Transactions on*, vol. 25, no. 1, pp. 124–136, Jan 2014.
- [10] G. Boracchi, M. Michaelides, and M. Roveri, "A cognitive monitoring system for contaminant detection in intelligent buildings," in *Neural Networks, International Joint Conference on*, July 2014, pp. 69–76.
- [11] P. Rodrigues, J. Gama, and J. Pedroso, "Hierarchical clustering of time-series data streams," *Knowledge and Data Engineering, IEEE Transactions on*, vol. 20, no. 5, pp. 615–627, May 2008.
- [12] V. Reppa, M. Polycarpou, and C. Panayiotou, "Decentralized isolation of multiple sensor faults in large-scale interconnected nonlinear systems," *Automatic Control, IEEE Transactions on*, vol. 60, no. 6, pp. 1582–1596, June 2015.
- [13] D. Fragkoulis, G. Roux, and B. Dahhou, "A global scheme for multiple and simultaneous faults in system actuators and sensors," in *Systems, Signals and Devices, 2009. SSD '09. 6th International Multi-Conference on*, March 2009, pp. 1–6.
- [14] L. Mhamdi, H. Dhouibi, N. Liouane, and Z. Simeu-Abazi, "Multiple fault diagnosis using mathematical models," in *Control Conference (ASCC), 2013 9th Asian*, June 2013, pp. 1–6.
- [15] C.-C. Li and J.-C. Jeng, "Multiple sensor fault diagnosis for dynamic processes," *ISA Transactions*, vol. 49, no. 4, pp. 415 – 432, 2010.
- [16] I. Issury and D. Henry, "A methodology for multiple and simultaneous fault isolation," in *Control Conference (ECC), 2009 European*, Aug 2009, pp. 2518–2523.
- [17] B. Pourbabaee, N. Meskin, and K. Khorasani, "Sensor fault detection, isolation, and identification using multiple-model-based hybrid kalman filter for gas turbine engines," *IEEE Transactions on Control Systems Technology*, vol. 24, no. 4, pp. 1184–1200, July 2016.
- [18] P. Arpaia, C. Manna, and G. Montenero, "Ant-search strategy based on likelihood trail intensity modification for multiple-fault diagnosis in sensor networks," *Sensors, IEEE*, vol. 13, no. 1, pp. 148–158, Jan 2013.
- [19] A. Sharma, H. Chen, M. Ding, K. Yoshihira, and G. Jiang, "Fault detection and localization in distributed systems using invariant relationships," in *Dependable Systems and Networks (DSN), 2013 43rd Annual IEEE/IFIP International Conference on*, June 2013, pp. 1–8.

TABLE I. EXPERIMENTAL RESULTS WITH MULTIPLE FAULTS WHERE THE PERCENTAGE OF AFFECTED SENSORS IS 5%.

	fault type	Proposed FDDS					FDDS in [6]				
		FP(%)	FN(%)	DD	ET (s)	RA(%)	FP(%)	FN(%)	DD	ET (s)	RA(%)
Syn.30	abrupt, $\alpha=0.15$	10.2	4.1	38.7	573.9	100	19.6	16.7	74.2	1128.4	100
	abrupt, $\alpha=0.3$	8.9	2.8	31.9	572.1	100	15.4	12.1	62.5	1121.5	100
	stack-at	2.1	4.5	28	573.9	100	7.9	31.9	64.1	1128.4	100
Syn.50	abrupt, $\alpha=0.15$	12.1	5.3	45.9	916	100	21.9	18.7	78.1	1865.8	100
	abrupt, $\alpha=0.3$	10.3	4.9	41.4	902.5	100	18.5	16.4	73.2	1753.3	100
	stack-at	5.3	4.5	31	902.6	100	7.3	15.6	39	1753.3	100
Rialba	abrupt, $\alpha=0.15$	6.2	6.5	16.7	289.3	100	7.8	8.6	61.4	321.8	100
	abrupt, $\alpha=0.3$	3.2	5.6	8.4	284.4	100	5.2	6.1	52.1	318.7	100
	stack-at	5.2	4.5	34.1	293.3	100	10.3	3.7	38.9	321.4	100
Wifi-U	abrupt, $\alpha=0.15$	6.3	6.7	36.8	837.5	100	8.9	7.5	47.1	1617.4	100
	abrupt, $\alpha=0.3$	5.1	5.9	31.9	819.8	100	8.1	6.4	40.1	1587.7	100
	stack-at	3.7	3.5	32.7	787.4	100	5.9	9.2	41.2	1512.8	100
Wifi-D	abrupt, $\alpha=0.15$	5.8	2.5	22.6	968.8	100	9.8	7.9	32.6	1229.1	100
	abrupt, $\alpha=0.3$	4.9	2.3	21.5	1120.4	100	8.3	7	29.4	1444	100
	stack-at	6.1	1.9	18.3	1132	100	10.9	5.5	28.9	1522.1	100

TABLE II. EXPERIMENTAL RESULTS WITH MULTIPLE FAULTS WHERE THE PERCENTAGE OF AFFECTED SENSORS IS 10%.

	fault type	Proposed FDDS					FDDS in [6]				
		FP(%)	FN(%)	DD	ET (s)	RA(%)	FP(%)	FN(%)	DD	ET (s)	RA(%)
Syn.30	abrupt, $\alpha=0.15$	8.1	3.6	36.7	402.5	100	16.3	16.1	76.4	697.6	100
	abrupt, $\alpha=0.3$	7.1	2.7	22.7	360.2	100	13.3	6.7	66.3	663.9	100
	stack-at	0.3	2.6	23.7	386	100	6.2	27.4	57.4	706.7	100
Syn.50	abrupt, $\alpha=0.15$	9.6	6.8	33.4	1411.3	100	17.4	18.5	78.2	2859.1	100
	abrupt, $\alpha=0.3$	8.3	5.9	31.6	1362.7	100	14.5	12.8	74.4	2936.6	100
	stack-at	3.8	3.3	28.5	1075.2	100	6.4	13.3	36.2	2871.8	100
Rialba	abrupt, $\alpha=0.15$	5.9	4.8	12.6	480.1	100	8.9	7.3	52.3	710.4	100
	abrupt, $\alpha=0.3$	2.4	3.7	6.3	472.5	100	3.5	4.7	46.8	703.6	100
	stack-at	6.7	1.2	23.3	469.3	100	8.7	1.8	32.9	690.4	100
Wifi-U	abrupt, $\alpha=0.15$	5.9	7.3	38.8	701.2	100	8.4	10.3	45.8	1360.2	100
	abrupt, $\alpha=0.3$	3.9	4	34.8	851.8	100	7.3	8.4	41.1	1590.5	100
	stack-at	3.9	4.4	35.7	709.2	100	5.4	6.1	49.3	1345.8	100
Wifi-D	abrupt, $\alpha=0.15$	3.1	7.5	68	1066.7	100	5.8	10.9	76.9	1403.9	100
	abrupt, $\alpha=0.3$	1.9	6.9	64.4	972.1	100	4.3	8.7	75.5	1302.4	100
	stack-at	1.9	7.1	67.1	959.4	100	4.3	9.7	74.2	1249.9	100

TABLE III. EXPERIMENTAL RESULTS WITH MULTIPLE FAULTS WHERE THE PERCENTAGE OF AFFECTED SENSORS IS 15%.

	fault type	Proposed FDDS					FDDS in [6]				
		FP(%)	FN(%)	DD	ET (s)	RA(%)	FP(%)	FN(%)	DD	ET (s)	RA(%)
Syn.30	abrupt, $\alpha=0.15$	7.8	3.3	34.5	590.7	100	15.3	13.2	73.1	1108.9	100
	abrupt, $\alpha=0.3$	6.4	2	19.6	544.3	100	11	6.1	57.6	1126.4	100
	stack-at	0.2	1.4	18.5	575.3	100	5.4	5.5	54.1	1118.9	100
Syn.50	abrupt, $\alpha=0.15$	9.1	5.9	31	934.9	100	16.8	17.3	68.9	1840	100
	abrupt, $\alpha=0.3$	8.3	4.2	28.1	919.2	100	14.1	15	59.1	1840.2	100
	stack-at	3.5	3.1	25.2	947.9	100	5.1	10.4	32.9	1813.2	100
Rialba	abrupt, $\alpha=0.15$	3.2	6	14.8	293.9	100	6.7	9	59.7	325.2	100
	abrupt, $\alpha=0.3$	2.5	5.1	8.6	291.3	100	4.2	6.3	42.1	320.7	100
	stack-at	7.1	1.5	13.8	295.4	100	9.1	2.3	34.6	342.4	100
Wifi-U	abrupt, $\alpha=0.15$	4.2	5.1	38.8	833.6	100	8.8	7.6	46.7	1597.1	100
	abrupt, $\alpha=0.3$	3.9	4.3	38	833.6	100	7.4	5.2	43.1	1597.1	100
	stack-at	3.9	4.7	35.2	849	100	7.3	6.8	47.9	1564.7	100
Wifi-D	abrupt, $\alpha=0.15$	2.1	6.9	65.3	1110.1	100	2.1	9.4	89.2	1444.4	100
	abrupt, $\alpha=0.3$	2	6.7	62.4	1110.5	100	2	9.5	95.2	1440.2	100
	stack-at	2	6.8	64.2	1093.1	100	2.1	9.3	86.9	1456.9	100

[20] Z. Du and X. Jin, "Multiple faults diagnosis for sensors in air handling unit using fisher discriminant analysis," *Energy Conversion and Management*, vol. 49, no. 12, pp. 3654 – 3665, 2008.

[21] M.-W. L. DING-SOU CHEN and J. LIU, "Isolating multiple sensor faults based on self-contribution plots with adaptive monitoring," *China Steel Technical Report*, no. 24, pp. 64–73, 2011.

[22] S. Altaf, A. Al-Anbuky, and H. GholamHosseini, "Fault diagnosis in a distributed motor network using artificial neural network," in *Power Electronics, Electrical Drives, Automation and Motion (SPEDAM), 2014 International Symposium on*, June 2014, pp. 190–197.

[23] C. Alippi, "Learning in nonstationary and evolving environments," in *Intelligence for Embedded Systems*. Springer International Publishing, 2014, pp. 211–247.

[24] L. Kaufman and P. Rousseeuw, "Clustering by means of medoids," in *Statistical Data Analysis Based on the L1-Norm and Related Methods*, Y. Dodge, Ed. North-Holland, 1987, pp. 405–416.

[25] S. Theodoridis and K. Koutroubas, *Pattern Recognition, Third Edition*. Orlando, FL, USA: Academic Press, Inc., 2006.

[26] L. Ljung, *System identification*. Wiley Online Library, 1999.

[27] C. Alippi, S. Ntalampiras, and M. Roveri, "An hmm-based change detection method for intelligent embedded sensors," in *IEEE International Joint Conference on Neural Networks*. IEEE, 2012.

[28] C. Alippi, R. Camplani, C. Galperti, A. Marullo, and M. Roveri, "A high-frequency sampling monitoring system for environmental and structural applications," *ACM Transactions on Sensor Networks (TOSN)*, vol. 9, no. 4, p. 41, 2013.

[29] —, "An hybrid wireless-wired monitoring system for real-time rock

TABLE IV. EXPERIMENTAL RESULTS WITH TIME VARIANCE WHERE THE PERCENTAGE OF AFFECTED SENSORS IS 30%.

	λ	Proposed FDDS					FDDS in [6]				
		FP(%)	FN(%)	DD	ET (s)	RA(%)	FP(%)	FN(%)	DD	ET (s)	RA(%)
Syn.30	0.05	8.3	5.1	13	1489.1	100	-	-	-	2983.5	-
	0.07	4.1	1.5	9	1427.7	100	-	-	-	2902.6	-
	0.1	2.7	0.9	6	1429.4	100	-	-	-	2887.6	-
Syn.50	0.05	8.7	5.6	15	6052.7	100	-	-	-	14517.3	-
	0.07	5.3	2.4	9	6588.4	100	-	-	-	8856	-
	0.1	2.5	1.4	7	6801.6	100	-	-	-	9895.4	-

TABLE V. EXPERIMENTAL RESULTS WITH TIME VARIANCE WHERE THE PERCENTAGE OF AFFECTED SENSORS IS 50%.

	λ	Proposed FDDS					FDDS in [6]				
		FP(%)	FN(%)	DD	ET (s)	RA(%)	FP(%)	FN(%)	DD	ET (s)	RA(%)
Syn.30	0.05	7.3	5	12.2	2113.8	100	23.5	22.7	54.2	2670.6	81.5
	0.07	3.9	3.6	9.5	2139.3	100	20.9	19.6	49.3	2700.5	85.4
	0.1	2.1	1.5	6.7	2101.4	100	18.9	17	45.7	2670.8	87.9
Syn.50	0.05	8.9	6.4	19	2512.1	100	24.9	23.3	59	3851.9	75.6
	0.07	7.5	5.3	14	1792.8	100	19.7	21.1	49.2	2816.9	84.3
	0.1	4.3	2.4	8	1802.1	100	16.5	18.2	45.3	2830.9	87.4

TABLE VI. EXPERIMENTAL RESULTS WITH TIME VARIANCE WHERE THE PERCENTAGE OF AFFECTED SENSORS IS 70%.

	λ	Proposed FDDS					FDDS in [6]				
		FP(%)	FN(%)	DD	ET (s)	RA(%)	FP(%)	FN(%)	DD	ET (s)	RA(%)
Syn.30	0.05	6.2	4.9	11.9	2403.5	100	21.9	20.1	50.9	2895.9	89.2
	0.07	3.1	2.9	8	2329.1	100	15.3	17.1	45.2	2603.7	92.1
	0.1	1.5	1.4	5.7	2343.9	100	12.4	16.9	42.9	2698	96.4
Syn.50	0.05	7.5	6.9	16.7	2165.6	100	22.9	21.4	52.2	3509.6	88.9
	0.07	6.3	5.1	12.6	2200.4	100	19.4	18.4	45.9	3511.7	91.9
	0.1	5.5	4.3	8.9	1792.4	100	14.5	17.3	43.5	2800.7	95.9

collapse forecasting” in *Mobile Adhoc and Sensor Systems, 2010 IEEE 7th International Conf. on.* IEEE, 2010, pp. 224–231.

- [30] M. Abdelghani and M. I. Friswell, “Sensor validation for structural systems with multiplicative sensor faults,” *Mechanical Systems and Signal Processing*, vol. 21, no. 1, pp. 270 – 279, 2007.



Cesare Alippi received the degree in electronic engineering cum laude in 1990 and the PhD in 1995 from Politecnico di Milano, Italy. Currently, he is a Full Professor with the Politecnico di Milano, Milano, Italy and Universit della Svizzera italiana, Lugano, Switzerland. He has been a visiting researcher at UCL (UK), MIT (USA), ESPCI (F), CASIA (RC), A*STAR (SIN), UKobe (JP). Alippi is an IEEE Fellow, Board of Governors member of the International Neural Network Society, Board of Directors member of the European Neural Network Society, Past Vice-

President education of the IEEE Computational Intelligence Society, past Associate editor of the IEEE Computational Intelligence Magazine, the IEEE-Transactions on Instrumentation and Measurements, the IEEE-Transactions on Neural Networks. In 2016 he received the Gabor award from the International Neural Networks Society and the IEEE Computational Intelligence Society Outstanding Transactions on Neural Networks and Learning Systems Paper Award; in 2013 the IBM Faculty award; in 2004 the IEEE Instrumentation and Measurement Society Young Engineer Award; in 2011 has been awarded Knight of the Order of Merit of the Italian Republic. Current research activity addresses adaptation and learning in non-stationary environments and Intelligence for embedded and cyber-physical systems. He holds 5 patents, has published one monograph book, 6 edited books and about 200 papers in international journals and conference proceedings.

Stavros Ntalampiras received the engineering and Ph.D. degrees from the Department of Electrical and Computer Engineering, University of Patras, Greece, in 2006 and 2010, respectively. Subsequently, he joined the System Architectures Group of the Department of Electronics and Information at Politecnico di Milano. From May 2013 to March 2015, he was conducting research with the Joint Research Center of the European Commission. Since April 2015 he is a Politecnico di Milano senior research fellow carrying out didactic and research activities. He has authored over 40 publications in peer-reviewed journals and conferences with more than 450 citations. He is a member of the IEEE Computational Intelligent Society Task Force on Computational Audio Processing, while his current research interests include content-based signal processing, fault diagnosis, audio pattern recognition, cyber physical systems, and critical infrastructure protection.



Manuel Roveri received the Dr.Eng. degree in Computer Science Engineering from the Politecnico di Milano (Milano, Italy) in June 2003, the MS in Computer Science from the University of Illinois at Chicago (Chicago, Illinois, U.S.A.) in December 2003 and the Ph.D. degree in Computer Engineering from Politecnico di Milano (Milano, Italy) in May 2007. Currently, he is an Associate Professor at the Dipartimento di Elettronica, Informazione e Bioingegneria of the Politecnico di Milano. His research interests include intelligent embedded systems, computational intelligence and adaptive algorithms. Manuel Roveri is an Associate Editor of the IEEE Transactions on Neural Networks and Learning Systems and served as chair and member in many IEEE subcommittees.